ORIGINAL ARTICLE

CrossMark

The "independent breath" algorithm: assessment of oxygen uptake during exercise

Maria Pia Francescato[1] · Valentina Cettolo[1]

Abstract

Purpose Reduction of noise of breath-by-breath gas-exchange data is crucial to improve measurements. A recently described algorithm ("independent breath"), that neglects the contiguity in time of breaths, was tested.

Methods Oxygen, carbon dioxide fractions, and ventilatory flow were recorded continuously over 26 min in 20 healthy volunteers at rest, during unloaded and moderate intensity cycling and subsequent recovery; oxygen uptake ($\dot{V}O_2$) was calculated with the "independent breath" algorithm (IND) and, for comparison, with three other "classical" algorithms. Average $\dot{V}O_2$ and standard deviations were calculated for steady-state conditions; non-linear regression was run throughout the $\dot{V}O_2$ data of the transient phases (ON and OFF), using a mono-exponential function.

Results Comparisons of the different algorithms showed that they yielded similar average $\dot{V}O_2$ at steady state ($p = $ NS). The standard deviations were significantly lower for IND (post hoc contrasts, $p < 0.001$), with the slope of the relationship with the corresponding data obtained from "classical" algorithms being < 0.69. For both transients, the overall kinetics (evaluated as time delay + time constant) was significantly faster for IND (post hoc contrasts, $p < 0.001$). For the ON transient, the asymptotic standard errors of the kinetic parameters were significantly lower for IND, with the slope of the regression line with the corresponding values obtained from the "classical" algorithms being < 0.60.

Conclusion The "independent breath" algorithm provided consistent average O_2 uptake values while reducing the overall noise of about 30%, which might result in the halving of the required number of repeated trials needed to assess the kinetic parameters of the ON transient.

Keywords Gas exchange · Signal-to-noise ratio · Mean response time

Abbreviations

ASE	Asymptotic standard error
AUC	"Auchincloss" approach, i.e., the breath-by-breath alveolar gas-exchange algorithm according to Auchincloss et al. (1966)
BTPS	Body temperature pressure saturated
EXP	"expiration-only" approach, i.e., the breath-by-breath gas-exchange algorithm that uses information obtained during expiration and the Haldane transformation (Roecker et al. 2005; Ward 2018)
FCO_2, FN_2, FO_2	Instantaneous carbon dioxide, non-exchangeable gas at alveolar level (essentially nitrogen) and oxygen fractions
FIO_2, FIN_2	Inspired oxygen and nitrogen ambient fractions

✉ Maria Pia Francescato
mariapia.francescato@uniud.it

[1] Department of Medicine, University of Udine, P.le Kolbe 4, 33100 Udine, Italy

IND	"independent breath" approach, i.e., the breath-by-breath alveolar gas-exchange algorithm under investigation (Cettolo and Francescato 2018b)
MANOVA	Repeated measures multivariate analysis of variance
MRT_{ON}, MRT_{OFF}	Mean response time of the ON and OFF kinetics, respectively
RSS	Residual sum of squares
STPD	Standard temperature pressure dry
t	Time
t_{df}	t student value for a determined degree of freedom at a certain probability level
Td_{ON}, Td_{OFF}	Time delay of the start of the ON and OFF kinetics, respectively
t_i, t_e	Starting times of inspiration and expiration, respectively; defined on the flow trace, where flow changes direction
T_{ON}, T_{OFF}	Start time of signal change of the ON and OFF transients, respectively, as obtained by the non-linear regression procedure
t_x	Time of the end-expiratory exchanged gas fraction, defined on the FO_2 trace
t_1, t_2	Start and end times of the jth breath for the "independent breath" approach; defined on the FO_2/FN_2 trace
$\dot{V}$	Respiratory flow at the mouth
V_L	End-expiratory lung volume
$\dot{V}O_2^{IND}$, $\dot{V}O_2^{WES}$, $\dot{V}O_2^{AUC}$, and $\dot{V}O_2^{EXP}$	Oxygen uptake calculated applying the "independent breath", the "Wessel", the "Auchincloss", and the "expiration-only" approaches, respectively; all the data are expressed in STPD conditions
$\dot{V}O_2^r$	Baseline O_2 uptake for the ON kinetic analysis
$\dot{V}O_2^{ss}$	Average steady-state O_2 uptake for the OFF kinetic analysis
WES	"Wessel" approach, i.e., the breath-by-breath alveolar gas-exchange algorithm according to Wessel et al. (1979)
$\Delta\dot{V}O_2^{rec}$	Fall of oxygen uptake at the end of recovery
$\Delta\dot{V}O_2^{ss}$	Increase in oxygen uptake at steady state
τ_{ON}, τ_{OFF}	Time constant of the ON and OFF responses, respectively, as obtained by the non-linear regression procedure

Introduction

Automated devices are currently available to assess gas exchange in humans. The hardware and software of these devices easily allow to measure gas exchange in real time with the highest possible temporal resolution (e.g., breath-by-breath). The algorithms applied for the calculations, however, are still a crucial point and the optimal one is lacking. Consequently, algorithms for breath-by-breath gas-exchange calculation that reduce the inherent fluctuations of data, i.e., noise, should be searched for.

The noise can be due to the exaggerated sensitivity of gas exchange to small errors in calibration and measurement (Beaver et al. 1981), but, even more, to the changes in lung gas stores (Capelli et al. 2011), which are accounted for in a few algorithms designed and implemented in the past years (Golja et al. 2018).

Recently, we proposed a new breath-by-breath gas-exchange calculation algorithm (Cettolo and Francescato 2018b) also theoretically able to account for the possible changes in lung gas stores. The algorithm is based on the alternative view of the respiratory cycle (Cettolo and Francescato 2015) which follows Grønlund's original approach (1984). The new algorithm (called "independent breath") processes each respiratory cycle in a completely independent way, i.e., each cycle is delimited without taking into account the end timepoint of the preceding cycle and/or the start time of the subsequent one.

The "independent breath" algorithm was preliminary tested under extreme conditions, namely, hyperventilation manoeuvres performed at rest by the volunteers (Cettolo and Francescato 2018b). During these manoeuvres, ventilation was disproportionate compared to the actual metabolic requirement and changes in lung gas stores definitely occurred, as confirmed

by the drastic changes in the end-tidal gas fractions between subsequent breaths (Cettolo and Francescato 2018a, b). This quick and huge phenomenon likely does not occur during exercise, not even during the transition between two different metabolic conditions.

A validation of the "independent breath" algorithm under steady-state moderate intensity exercise, where a low signal-to-noise ratio is usually observed, is lacking, as well as during exercise transient phases. Notably, transients create changes in ventilation that are not necessarily precisely matched to changes in transmembrane oxygen flow; thus, there are reasons to suspect that the gas-exchange data obtained during transient are more sensitive to the algorithm applied for their calculation.

The aim of the present work was thus to evaluate the performance of the "independent breath" algorithm (Cettolo and Francescato 2018b) adopting an exercise protocol that allowed us to analyse both the steady-state conditions and the transient phases. As far as a recognized reference method does not exist (Ward 2018), a comparison with results provided by "classical" real-time breath-by-breath algorithms commonly applied by other laboratories (Golja et al. 2018) was also performed. Accordingly, gas-exchange data were calculated by means of the algorithms of Auchincloss et al. (1966), of Wessel et al. (1979), and of the algorithm that uses only information obtained during expiration, associated with the Haldane transformation (Roecker et al. 2005; Ward 2018).

Methods

Subjects

Twenty healthy and moderately active adults (10 males and 10 females) were thoroughly informed of the nature, purpose, and possible risks and gave their written consent to participate in the study.

Average ($\pm$ SD) age of volunteers was 40.0 ± 13.7 years; they were 1.74 ± 0.11 m tall and had a body mass of 70.4 ± 12.9 kg. Functional residual capacity, estimated for each volunteer based on anthropometrical data (Roberts et al. 1991), amounted on average to 3.3 ± 0.6 L.

The local Ethical Committee of the Friuli-Venezia Giulia (Italy) region approved the study, which was conducted also according to the Declaration of Helsinki.

Experimental protocol

Upon arrival in the laboratory, volunteers were equipped with the belt of the heart rate monitor (Polar, Finland) and the facemask and then sat quietly on the bicycle ergometer (Excalibur Sport; Lode B.V., The Netherlands).

The trial consisted of four consecutive steps (Fig. 1): (a) 5 min at rest, sitting quietly on the ergometer; (b) 5 min pedalling without load (zero-load pedalling); (c) 6 min pedalling at 1 W kg^{-1} body mass; and (d) 10 min recovery (remaining seated quietly on the ergometer); consequently, overall duration was 26 min (i.e., 1560s). Timings of the trial and workloads were controlled, and automatically recorded by the metabolic unit; during the two pedalling periods, volunteers were asked to maintain the pedalling frequency as close as possible to 60 rpm with the aid of the values shown on the control unit.

Respiratory flow ($\dot{V}$), O_2 and CO_2 fractions (FO_2 and FCO_2, respectively) at the mouth were continuously recorded during the trial (CPET Metalyzer 3B, Cortex, Germany). Gases were sampled through a $\sim$ 2 m long capillary line inserted in the outer frame of the flow meter and analysed by fast-response electro-chemical O_2 and infra-red CO_2 sensors embedded in the metabolic cart. The software operating the metabolic unit allowed the recording of gas fractions, and flow signal, then saving them as text files with a sampling frequency of 50 Hz. Traces of gas fractions and flow were temporally synchronized by the firmware of the metabolic unit, which also converted flow to BTPS conditions. Before each test, following the procedures indicated by the manufacturer, the analysers were calibrated with a gas mixture of known composition ($FO_2 = 16.0\%$; $FCO_2 = 4.0\%$; FN_2 as balance) and ambient air; the flow meter was calibrated by means of a 3 L syringe (Cortex, Germany).

Data treatment

For all the volunteers, breath-by-breath oxygen uptake was calculated from the original gas fractions and flow traces by means of all the algorithms under investigation, i.e.,
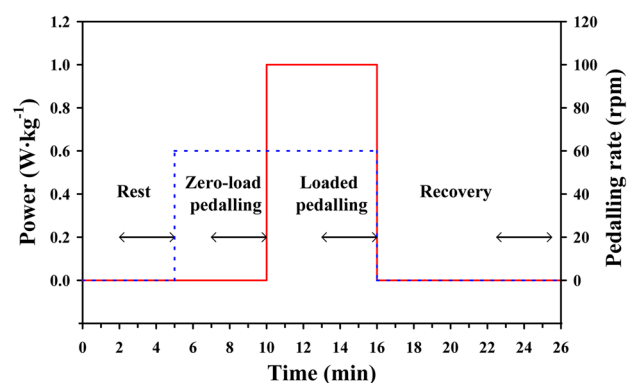

Fig. 1 Schematic representation of the experimental protocol. Continuous line illustrates the imposed mechanical work; dotted line is the pedalling frequency. Segments limited by arrows represent the time intervals analysed as steady-state conditions

the "independent breath" approach (IND), the "Wessel" approach (WES), the "Auchincloss" approach (AUC), and the "expiration-only" approach (EXP), respectively. As a result, four oxygen uptake time series were obtained for each volunteer ($\dot{V}O_2^{IND}$, $\dot{V}O_2^{WES}$, $\dot{V}O_2^{AUC}$, and $\dot{V}O_2^{EXP}$, respectively). No data were discarded on all the time series before any of the subsequent analyses.

Common assumptions

Computerized procedures were specifically developed in C language under the Unix-like Cygwin environment (Red Hat Cygwin, version 4.3.39); the same files containing the oxygen and carbon dioxide fractions and flow traces, as yielded by the metabolic cart, were used to calculate the gas exchange according to the four investigated algorithms.

The value of one minus the sum of measured O_2 and CO_2 fractions was assumed to represent only the gases not exchanged at alveolar level and was labelled FN_2 being essentially composed of nitrogen. All the calculated data were converted to STPD conditions. To avoid incoherent data, the respiratory cycles were considered valid only if the inspiratory and/or the expiratory volumes were greater a theoretical dead space, assumed to be of at most 150 mL (Fowler 1948); if not, the invalid breath was incorporated with the following one.

To delimit each respiratory cycle by its own, the following procedure is applied:

1. The minimum end-expiratory FO_2/FN_2 ratio is searched for the jth breath as well as for the preceding expiration.
2. The higher of the two FO_2/FN_2 values found at point 1 is used as reference ratio.
3. Going backwards from the end of the expiration of the jth breath, the first timepoint, where the FO_2/FN_2 ratio corresponds to the reference ratio (as set in point 2), is assumed as the end timepoint of the respiratory cycle ($t_{2,j}$).
4. Going backwards from the end of the preceding expiration, the first timepoint, where the FO_2/FN_2 ratio corresponds to the reference ratio (as set in point 2), is assumed as the start timepoint of the respiratory cycle ($t_{1,j}$).

The "Auchincloss" and "Wessel" approaches

The theory underlying the algorithms believed to account for the changes in lung gas stores was described in depth by Auchincloss et al. (1966). The final general equation for the jth breath can be written as

$$\dot{V}O_{2j} = -\frac{\int_{t_{i,j-1}}^{t_{i,j}} \dot{V} \cdot FO_2 \, dt - \frac{FO_2(t_{x,j})}{FN_2(t_{x,j})} \cdot \int_{t_{i,j-1}}^{t_{i,j}} \dot{V} \cdot FN_2 \, dt - V_L \cdot FN_2(t_{x,j-1}) \cdot \left\{ \frac{FO_2(t_{x,j})}{FN_2(t_{x,j})} - \frac{FO_2(t_{x,j-1})}{FN_2(t_{x,j-1})} \right\}}{t_{i,j} - t_{i,j-1}}, \tag{2}$$

The "independent breath" approach

Main characteristic of this approach is that the start and end points of the respiratory cycle are identified based on equal expiratory FO_2/FN_2 ratios, which makes the knowledge of lung volume at the beginning of the breath unnecessary for the calculation of breath-by-breath gas exchange. The integration interval of the "independent breath" approach is identified on the trace of the FO_2/FN_2 ratio. The equation used to calculate the O_2 uptake for the jth breath is the following:

$$\dot{V}O_{2j}^{IND} = -\frac{\int_{t_{1,j}}^{t_{2,j}} \dot{V} \cdot FO_2 \, dt - \frac{FO_{2j}(t_{1,j})}{FN_{2j}(t_{1,j})} \cdot \int_{t_{1,j}}^{t_{2,j}} \dot{V} \cdot FN_2 \, dt}{t_{2,j} - t_{1,j}}. \tag{1}$$

As described previously in detail (Cettolo and Francescato 2018b), the "independent breath" approach delimits each respiratory cycle without taking into account the end timepoint of the preceding cycle and/or the start time of the subsequent one, hence independently (Fig. 2).

where FO_2 and FN_2 are the instantaneous oxygen and "nitrogen" fractions, as assessed at the mouth; time $t_{i,j}$ corresponds to the timepoint, where the flow changes direction and the inspiration starts and $t_{x,j}$ is the timepoint corresponding to the end-expiratory gas fraction (Fig. 2). In turn, V_L is the end-expiratory lung volume.

According to the algorithm proposed by Auchincloss et al. (1966), the O_2 uptake ($\dot{V}O_2^{AUC}$) is calculated assuming that V_L corresponds to subject's functional residual capacity; in the present work, functional residual capacity was estimated from anthropometrical data (Roberts et al. 1991).

Wessel et al. (1979) completely neglected the third part of the Eq. (2), which is tantamount saying that the O_2 uptake ($\dot{V}O_2^{WES}$) is calculated assuming a V_L equal to 0 L.

The "expiration-only" approach

To calculate the O_2 uptake during the jth breath using information obtained only during expiration and then applying the Haldane transformation (Roecker et al. 2005; Ward
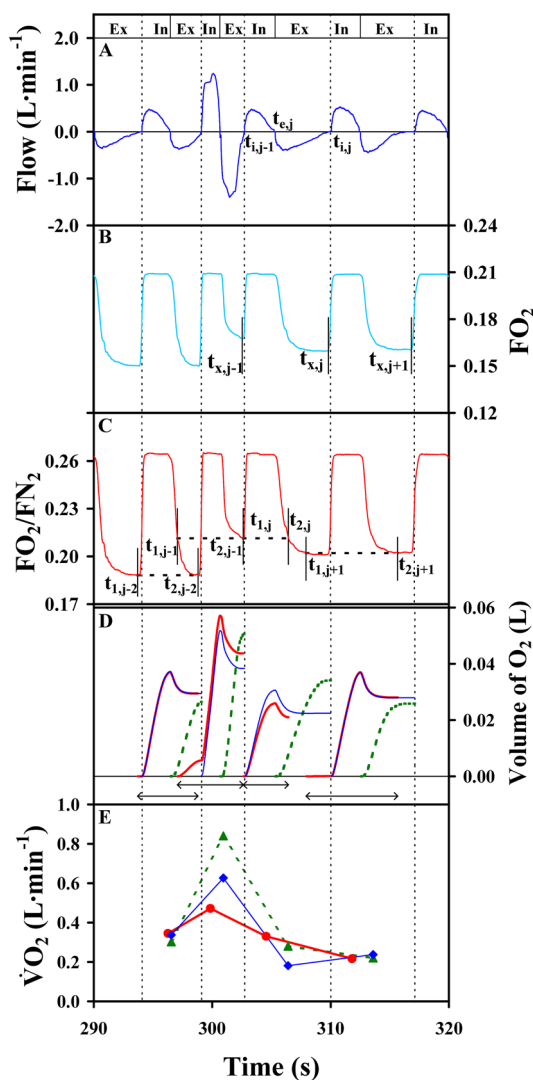
Fig. 2 Raw data for a few consecutive breaths, and corresponding data treatment results, as a function of time. **a, b** Flow and O_2 fraction traces, as recorded at the mouth. Times $t_{i,j}$ and $t_{e,j}$ correspond to the timepoints, where the flow changes direction, thus where inspiration and expiration start, respectively; according to the classical view of the respiratory cycle, the period between $t_{i,j-1}$ and $t_{i,j}$ corresponds to the duration of the jth breath. The timepoints corresponding to the end-expiratory gas fractions ($t_{x,j}$) are also illustrated. **c** Trace of the ratio between O_2 and "nitrogen" fractions. This trace is used by the "independent breath" approach to identify the start ($t_{1,j}$) and end ($t_{2,j}$) timepoints of the jth breath; the period between $t_{1,j}$ and $t_{2,j}$ corresponds to the duration of the jth breath. **d** Integrals of O_2 volume as obtained using the following algorithms: "independent breath" (thick continuous line), "Wessel" (thin continuous line), and "expiration-only" (dotted line). The time intervals over which the integrals are calculated are: highlighted by the arrows for the IND approach, between two subsequent start of inspiration for the WES approach, and only expiration for the EXP approach. **e** O_2 uptakes calculated by means of the following algorithms: "independent breath" (dots and thick line), "Wessel" (diamonds and thin line), and "expiration-only" (triangles and dotted line). Timings of the O_2 uptakes are referred to the central timepoint of the corresponding respiratory cycle; this last corresponds to the time interval of its integration for the IND approach, whereas it corresponds to the time interval between two successive start of inspiration for the WES and EXP approaches. Vertical dotted lines are the start of inspirations. *In* inspiration, *Ex* expiration

2018), i.e., using the "expiration-only" approach ($\dot{V}O_2^{EXP}$), the following equation is used:

$$\dot{V}O_{2j}^{EXP} = -\frac{\int_{t_{e,j}}^{t_{i,j}} \dot{V} \cdot FO_2 \, dt - \frac{FIO_2}{FIN_2} \cdot \int_{t_{e,j}}^{t_{i,j}} \dot{V} \cdot FN_2 \, dt}{t_{i,j} - t_{i,j-1}}, \quad (3)$$

where FO_2 and FN_2 are the instantaneous oxygen and "nitrogen" fractions, as assessed at the mouth; times $t_{i,j}$ and $t_{e,j}$ correspond to the timepoints, where the flow changes direction and the inspiration and expiration start, respectively (Fig. 2); FIO_2 and FIN_2 correspond to the inspired ambient fractions and were set to 20.93% and 79.02%, respectively.

Data analysis

The adopted experimental protocol allowed us to investigate both steady-state conditions and transients.

For all the four O_2 uptake time series ($\dot{V}O_2^{IND}$, $\dot{V}O_2^{WES}$, $\dot{V}O_2^{AUC}$, and $\dot{V}O_2^{EXP}$) of each volunteer, steady-state average values, and corresponding standard deviations (SD), were calculated over 4 time periods (Fig. 1). In more detail, the latter were: (a) at rest (from min 2:00 to min 5:00); (b) during zero-load pedalling (from min 7:00 to min 10:00); (c) during loaded pedalling (from min 13:00 to min 16:00); and (d) at the end of recovery (from min 22:30 to min 25:30).

In addition, for all the time series ($n = 4 \times 20$), the two main transients were analysed. The non-linear regression procedure was run as previously described (Francescato et al. 2014b) using the statistical environment R (version 3.2.2; R Core Team 2015) with the standard R libraries and the *minpack.lm* library. The best fit was defined by minimization of the sum of the vertical distances between data points and the fitted curve, i.e., of the residual sum of squares (RSS; Bates and Watts 1988; Motulsky and Ransnas 1987). The software running the non-linear regression procedure returned the RSS values, together with the estimated parameters along with their asymptotic standard error (ASE). Notably, the ASE is the statistical basis to obtain, for each estimated parameter, the width of its confidence interval (Francescato et al. 2014a, b), which is calculated as $\pm t_{df} \times ASE$. In turn, t_{df} is the t student value for a determined degree of freedom at a certain probability level. For a probability level of 95% and a degree of freedom > 60, t_{df} is < 2.0.

The following first-order function of time t was used to describe the oxygen uptake response during the zero-load-to-loaded pedalling transient (ON transient):

$$\dot{V}O_2(t) = \dot{V}O_2^r + \Delta\dot{V}O_2^{ss} \cdot \left(1 - e^{-\frac{t-T_{ON}}{\tau_{ON}}}\right). \quad (4)$$

The fitting procedure yielded the estimated values for: τ_{ON} (i.e., the time constant of the response), T_{ON} (i.e., the

start time of signal change), and $\Delta \dot{V}O_2{}^{ss}$ (i.e., the increase in oxygen uptake at steady state). $\dot{V}O_2{}^r$ was set to the average value over the 3 min zero-load pedalling before the start of work (i.e., 7:00 min $< t <$ 10:00 min). All the data within $t >$ 10:00 min (i.e., 600 s, without discarding any of the values after the start of the loaded exercise) and $t <$ 16:00 min (i.e., the end of loaded exercise), were considered for the fitting procedure. The time delay of the start of the kinetics (Td_{ON}) was calculated by subtracting the start time of the step change in mechanical power output from the estimated T_{ON}, i.e., $Td_{ON} = T_{ON} - 600$ s; the mean response time (MRT_{ON}) of the kinetics was then calculated as: $MRT_{ON} = Td_{ON} + \tau_{ON}$.

The oxygen uptake response during the loaded pedalling to rest transient (OFF transient) was described by the following first-order function of time t:

$$\dot{V}O_2(t) = \dot{V}O_2{}^{ss} - \Delta\dot{V}O_2{}^{rec} \cdot \left(1 - e^{-\frac{t - T_{OFF}}{\tau_{OFF}}}\right). \qquad (5)$$

The fitting procedure yielded the estimated values for: τ_{OFF} (i.e., the time constant of the response), T_{OFF} (i.e., the start time of signal change), and $\Delta\dot{V}O_2{}^{rec}$ (i.e., the fall of oxygen uptake at the end of recovery); in turn, $\dot{V}O_2{}^{ss}$ was set to the average value over the last 3 min steady-state exercise (i.e., 13:00 min $< t <$ 16:00 min). All the data with $t >$ 16:00 min (i.e., 960 s) were considered for the fitting procedure (without discarding the data pertaining to the initial seconds of recovery), corresponding to the whole recovery period lasting 10 min. The time delay of the start of the kinetics (Td_{OFF}), similar to the ON transient, was calculated by subtracting the stop time of the mechanical power from the estimated T_{OFF}, i.e., $Td_{OFF} = T_{OFF} - 960$ s; the mean response time (MRT_{OFF}) of the kinetics was then calculated as: $MRT_{OFF} = Td_{OFF} + \tau_{OFF}$.

Statistical analysis

Statistical analyses were performed using the SPSS software (Chicago, Ill., USA); results were expressed, as means $\pm$ SD and significance level was set to $p <$ 0.05.

Normal distribution was verified for all the variables by means of the Shapiro–Wilk test.

Because of the large fluctuations in the calculated gas-exchange data (see Fig. 3), results yielded by the Auchincloss's algorithm were discarded before performing the comparisons among the other algorithms at stake.

For the steady-state data, a repeated measure 3×4 within subjects factors Multivariate Analysis of Variance (MANOVA) was used to detect differences among the three investigated algorithms (algorithm effect) and the four different conditions (condition effect). For the ON transient, as well as for the OFF

transient, repeated measures MANOVA was used to compare the estimated kinetic parameters, corresponding ASE values, and RSS values provided by the non-linear regression procedure applied on the three different $\dot{V}O_2$ time series of the same volunteer (algorithm effect). In either case, Mauchly's test was used to check if the sphericity assumption appeared to be violated; if Mauchly's test was significant, the Huynh–Feldt ε was used to adjust the degrees of freedom. Post hoc simple contrast (against the "independent breath" algorithm or against the resting condition, as appropriate) was used to detect significant differences inside the within subjects effects.

Since some of the variables failed in showing a normal distribution, non-parametric statistical tests (two-sided Friedman tests) were also run, which confirmed all the statistically significant differences observed applying the MANOVA tests.

Correlation between variables was assessed by means of the Pearson's correlation coefficient and the least-squares method was applied to calculate the slopes and intercepts of the regression lines, together with the corresponding widths of the 95% confidence intervals and statistical significance levels. In addition, Bland and Altman's limits-of-agreement plot (Bland and Altman 1986) was used to assess the agreement between the investigated algorithms.

Post hoc analysis carried out on the main outcome of the study, i.e., the standard deviation of the oxygen uptakes during loaded exercise as obtained for the four algorithms, revealed a power of 0.99 for a correlation between groups of 0.80 (that yielded an effect size $>$ 0.95), and assuming a two tailed α error $<$ 0.01.

Results

Figure 3 illustrates, for one volunteer, the O_2 uptake obtained applying the four algorithms at stake. The four panels show the same behaviour of O_2 uptake as a function of time, although different levels of noise can be noted. Similar trends were obtained for all the volunteers.

Analysis of the steady-state conditions

Table 1 summarizes the grand averages of oxygen uptake calculated for the four steady-state conditions (i.e., rest, zero-load pedalling, loaded pedalling, and end of recovery) on the time series provided by the four algorithms at stake, together with the averages of the corresponding standard deviations.

The mean oxygen uptakes yielded by the "independent breath", the "Wessel" and the "expiration-only" algorithms during the four steady-state conditions were not significantly different (algorithm effect, $F = 0.617$, $p =$ NS); in turn, the four steady-state conditions showed significantly different
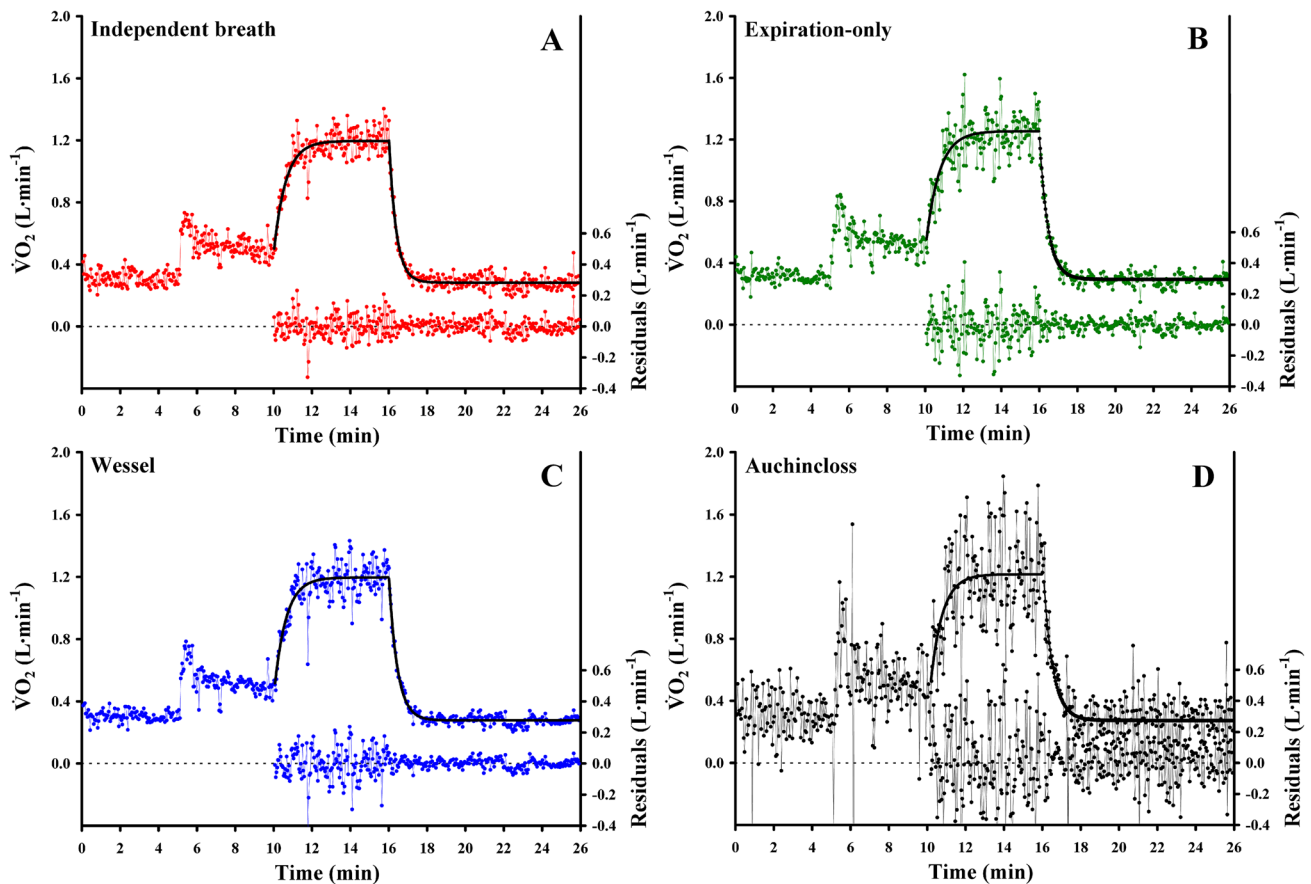
Fig. 3 O_2 uptake data obtained for one volunteer applying the "independent breath" (**a**), the "expiration-only" algorithm (**b**), the "Wessel" algorithm (**c**), and the "Auchincloss" algorithm (**d**); the same original flow and gas fraction traces were used for all the algorithms.

The "best-fit" response profiles for both the ON and OFF transients and for all the shown algorithms are illustrated as continuous lines; corresponding residuals are plotted below (right axis)

average values (condition effect, $F = 485.2$, $p < 0.001$). Post hoc contrasts revealed that rest and the end of recovery were not significantly different ($F = 0.205$, $p = NS$); conversely, both the zero-load pedalling and the loaded pedalling conditions showed significantly higher values as compared to rest ($F > 324.5$, $p < 0.001$). Similar results were obtained also for carbon dioxide exhalation (see table in Supplemental Material).

Figure 4a and b illustrates the linear regressions between the average steady-state $\dot{V}O_2^{WES}$ values (or the average $\dot{V}O_2^{EXP}$ values) and the corresponding average steady-state $\dot{V}O_2^{IND}$ values; in both cases, the points lie close to the identity line ($R > 0.997$, $p < 0.01$, and $n = 80$ for both correlations). The corresponding Bland–Altmann plots are shown in Fig. 4c and d; in both cases, the mean difference (i.e., the bias) was $< |4.0 \text{ mL min}^{-1}|$. The 95% limits of agreement of the differences with the "expiration-only" values (i.e., the worst case) were $+65.7$ and $-57.9 \text{ mL min}^{-1}$; the 95% limits of agreement with the "Wessel" algorithm were about

fourfold narrower; no relationship was observed between the differences and the corresponding average values.

The analysis on the standard deviations calculated for the same four steady-state time periods as above (Table 1) showed that they were significantly different among the time series provided by the three algorithms under comparison (algorithm effect, $F = 9.88$, $p < 0.001$). Post hoc analysis showed that the smallest standard deviations were those of $\dot{V}O_2^{IND}$ as compared to the other two time series (post hoc contrast, $F > 7.40$, $p < 0.05$). A significant difference was observed among the four steady-state investigated conditions (condition effect, $F = 20.5$, $p < 0.001$). The zero-load and the loaded pedalling conditions showed significantly greater standard deviations (post hoc contrast, $F > 7.29$, $p < 0.05$) as compared to rest and/or the end of recovery, in turn not significantly different each other (post hoc contrast, $F = 0.545$, $p = NS$). Figure 5 illustrates the standard deviations obtained for the data provided by the "independent breath" algorithm for all volunteers and all steady-state conditions as a function of the corresponding values obtained for the $\dot{V}O_2^{WES}$ and

Table 1 Average steady-state O_2 uptake values and corresponding standard deviations obtained using the time series yielded by the four algorithms at stake

	Time series			
	Independent breath	Auchincloss	Wessel	Expiration-only
Rest				
Mean (L min^{-1})	0.320 ± 0.075	0.321 ± 0.077	0.317 ± 0.074	0.307 ± 0.079
SD (L min^{-1})	0.057 ± 0.026	0.184 ± 0.122	0.059 ± 0.033*	0.065 ± 0.030***
Zero-load pedalling				
Mean (L min^{-1})	0.574 ± 0.109	0.568 ± 0.112	0.573 ± 0.112	0.575 ± 0.113
SD (L min^{-1})	0.076 ± 0.030	0.258 ± 0.122	0.084 ± 0.032*	0.090 ± 0.038***
Loaded pedalling				
Mean (L min^{-1})	1.224 ± 0.235	1.234 ± 0.237	1.230 ± 0.235	1.243 ± 0.244
SD (L min^{-1})	0.100 ± 0.044	0.293 ± 0.151	0.140 ± 0.068*	0.132 ± 0.051***
Recovery				
Mean (L min^{-1})	0.310 ± 0.087	0.305 ± 0.087	0.306 ± 0.087	0.318 ± 0.099
SD (L min^{-1})	0.062 ± 0.031	0.176 ± 0.084	0.060 ± 0.032*	0.071 ± 0.034***

$n = 20$ overall

*, **, and ***Significantly different from $\dot{V}O_2^{IND}$ time series (post hoc simple contrast) at the following significance levels: $p < 0.05$, $p < 0.01$, and $p < 0.005$, respectively. Notably, results obtained for the "Auchincloss" algorithm were not included in the statistical analysis of comparison between algorithms; see "Methods" for details

the $\dot{V}O_2^{EXP}$ time series. The correlation between the two variables was statistically significant ($R > 0.849$, $p < 0.001$, $n = 80$) in both cases, although the regression lines were far from the identity line. Indeed, the slope of the linear regression between the paired data amounted to 0.57 and 0.69, respectively; these values are significantly lower than the unit in both cases ($t > 7.27$, $p < 0.001$); the intercepts were significantly different from zero in both cases ($t > 2.85$, $p < 0.01$).

Analysis of the transients

Overlapping on the O_2 uptakes calculated for one subject, Fig. 3 shows the ON and OFF "best-fit" response profiles for all the used algorithms, and, below, the corresponding residuals. It appears that the residuals are generally smaller for the IND algorithm compared to the other three algorithms. A similar behaviour was observed for all the volunteers.

Table 2 summarizes the averages of the kinetic parameters and of the RSS values (i.e., the sum of the squares of the vertical distances between data points and fitted curve), as estimated by means of the non-linear regression procedure. Results for both the ON and OFF transients (i.e., the zero-load to loaded pedalling transient and the loaded pedalling to rest transient, respectively), obtained using the O_2 uptake time series provided by the four algorithms at stake ($\dot{V}O_2^{AUC}$, $\dot{V}O_2^{WES}$, $\dot{V}O_2^{IND}$, and $\dot{V}O_2^{EXP}$, respectively) are reported.

For both transients, the mean response time was significantly different when the $\dot{V}O_2$ data provided by the WES, IND, and EXP algorithms were used (algorithm effect, $F > 9.64$, $p < 0.001$ for both transients). Post hoc simple contrasts revealed that, in both transients, the $\dot{V}O_2^{IND}$ time series resulted in a shorter MRT as compared to the MRTs yielded by the $\dot{V}O_2$ time series provided by the other two algorithms ($F > 12.34$, $p < 0.005$ for the ON transient and $F > 25.55$, $p < 0.001$ for the OFF transient, respectively). Interestingly, no significant difference was detected among the time constants of the ON transient obtained using the $\dot{V}O_2^{WES}$, $\dot{V}O_2^{IND}$, and $\dot{V}O_2^{EXP}$ time series (algorithm effect, $F = 0.98$, $p = NS$), whereas the time delays were significantly different (algorithm effect, $F = 10.34$, $p < 0.001$), the $\dot{V}O_2^{IND}$ time series providing significantly shorter Td_{ON} (Post hoc simple contrast, $F > 10.50$, $p < 0.005$). As concerns the OFF transient, τ_{OFF} was significantly different when using the time series of the three algorithms under comparison (algorithm effect, $F = 7.43$, $p < 0.005$), the $\dot{V}O_2^{IND}$ data providing significantly shorter time constants (Post hoc simple contrast, $F > 8.70$, $p < 0.01$); conversely, no significant difference was detected among the Td_{OFF} (algorithm effect, $F = 0.17$, $p = NS$).

The RSS values were significantly different among the $\dot{V}O_2^{WES}$, $\dot{V}O_2^{IND}$ and $\dot{V}O_2^{EXP}$ time series either for the ON and the OFF transients (algorithm effect, $F > 10.90$, $p < 0.001$ for both transients). For the ON transient, the RSS values were lower when the fitting procedure was run on the $\dot{V}O_2^{IND}$ time series as compared to the other 2 time series (Post hoc simple contrast, $F > 16.34$, $p < 0.001$). Conversely, the use of the $\dot{V}O_2^{IND}$ time series in the OFF transient resulted in a lower RSS values only in comparison with the $\dot{V}O_2^{EXP}$ time series (post hoc simple contrast, $F = 13.37$, $p < 0.005$).
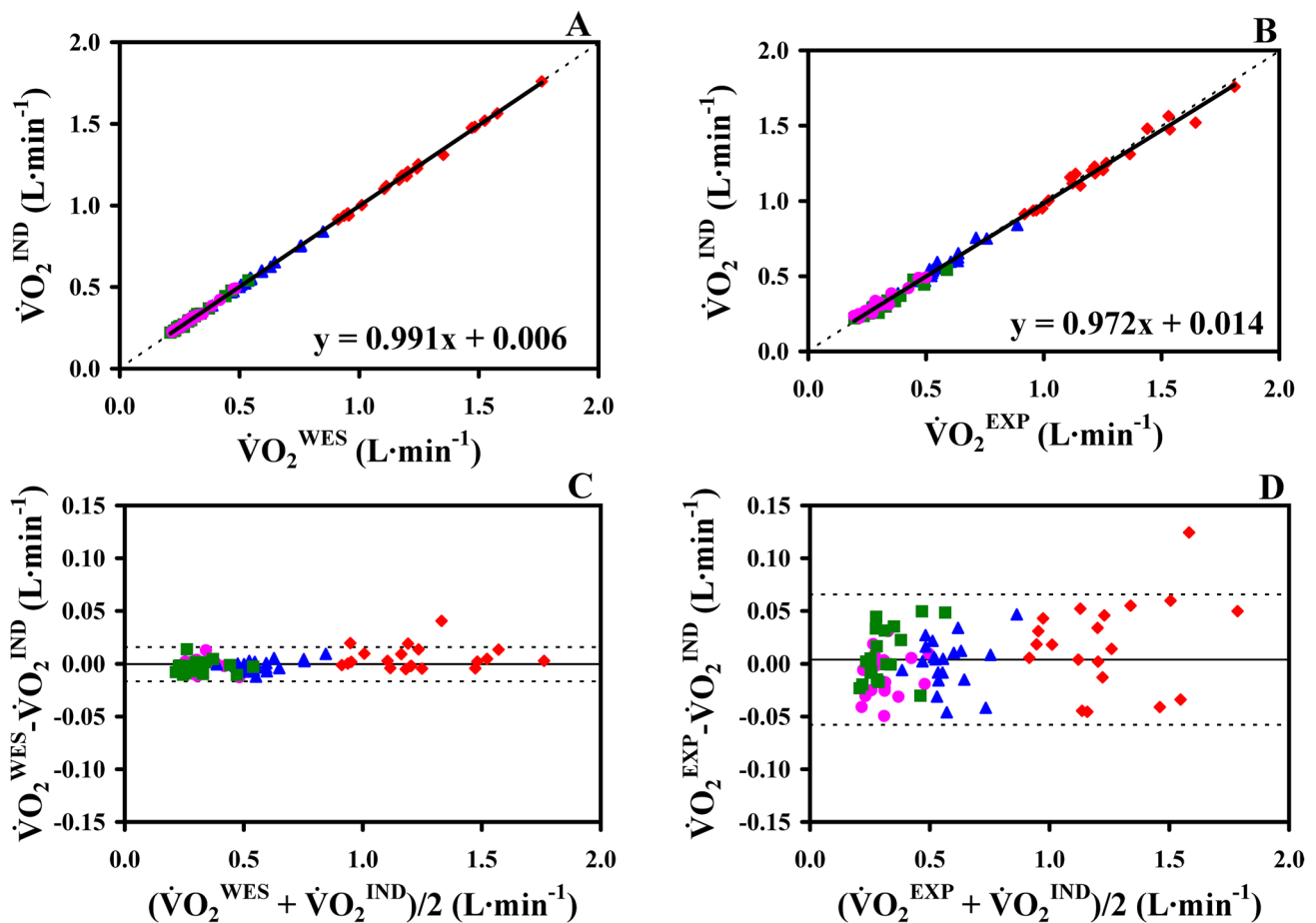
Fig. 4 Correlations between the average steady-state O_2 uptakes of the four investigated conditions as obtained from the $\dot{V}O_2^{IND}$ and the $\dot{V}O_2^{WES}$ time series (**a**) or the $\dot{V}O_2^{EXP}$ time series (**b**). The corresponding Bland–Altmann plots are illustrated in **c**, **d**. Data of all the 20 volunteers are plotted. In **a**, **b**, the continuous lines are the corresponding regression lines; dotted lines are the identity lines. In **c**, **d**, the continuous lines represent the bias, and dotted lines are the 95% limits of agreement. The data corresponding to the four steady-state conditions are illustrated with different symbols: filled circle ≡ rest; filled triangle ≡ zero-load pedalling; filled diamond ≡ steady-state exercise; filled square ≡ recovery

The ASE values of the estimated time constants and time delays were significantly different among the $\dot{V}O_2^{WES}$, $\dot{V}O_2^{IND}$, and $\dot{V}O_2^{EXP}$ time series either for the ON and the OFF transients (algorithm effect, $F > 6.87$, $p < 0.01$ for all). Post hoc simple contrasts revealed that, for both kinetic parameters of the ON transient, the ASE values were significantly lower for the $\dot{V}O_2^{IND}$ time series as compared to both the $\dot{V}O_2^{WES}$ and $\dot{V}O_2^{EXP}$ time series ($F > 10.32$, $p < 0.005$). Conversely, for the OFF transient, the $\dot{V}O_2^{IND}$ time series resulted in lower ASE values in comparison only with the $\dot{V}O_2^{EXP}$ time series ($F > 7.33$, $p < 0.05$). Figure 6 illustrates the individual ASE values obtained for the time constant (panels A and B) and for the time delay (panels C and D) using the $\dot{V}O_2^{IND}$ time series as a function of the corresponding ASE values obtained using the $\dot{V}O_2^{WES}$ (panels A and C) or the $\dot{V}O_2^{EXP}$ (panels B and D) time series. The ASE values

obtained for the ON and OFF transients are illustrated in the same panel. The correlation between the couples of data was statistically significant for all the conditions ($R > 0.639$, $p < 0.005$, $n = 20$). The slopes of the regression lines between paired data were in the range between 0.33 and 0.77, independent of the transient phase; these values are significantly lower than the unit in all the cases ($t > 2.19$, $p < 0.05$).

Discussion

The aim of the present work was to evaluate the performance of the "independent breath" algorithm, focusing in particular on its noise. Main result was that the "independent breath" algorithm provided significantly lower noise in the O_2 uptake values compared to the other
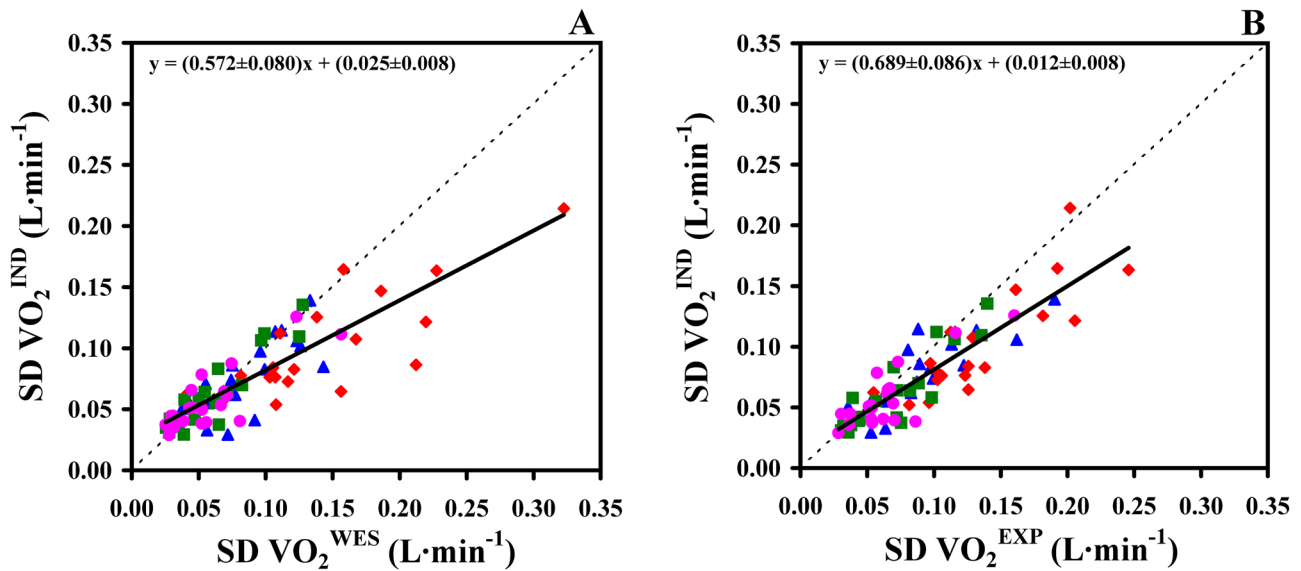
Fig. 5 Correlation between the standard deviations (SD) calculated for the O_2 uptakes provided by the "independent breath" and the "Wessel" algorithms for the four investigated steady-state conditions (**a**); **b** illustrates the same correlation for the "expiration-only" algorithm. Data of all the 20 volunteers are plotted. Continuous lines are the corresponding regression lines; dotted lines are the identity lines. The data corresponding to the four steady-state conditions are illustrated with different symbols: filled circle ≡ rest; filled triangle ≡ zero-load pedalling; filled diamond ≡ steady-state exercise; filled square ≡ recovery

Table 2 Average estimated parameters and RSS values obtained for the ON and OFF transients using the $\dot{V}O_2^{IND}$, $\dot{V}O_2^{AUC}$, $\dot{V}O_2^{WES}$, or $\dot{V}O_2^{EXP}$ time series

	Transient	Time series			
		"Independent breath"	"Auchincloss"	"Wessel"	"Expiration-only"
Time constant					
τ_{ON} (s)	ON	52.4 ± 17.9	53.1 ± 19.3	53.6 ± 18.9	54.6 ± 18.6
τ_{OFF} (s)	OFF	38.7 ± 9.9	42.4 ± 11.4	41.0 ± 10.4**	41.6 ± 10.1***
Time delay					
Td_{ON} (s)	ON	4.9 ± 4.2	11.7 ± 5.8	8.1 ± 5.0***	7.2 ± 5.0***
Td_{OFF} (s)	OFF	1.0 ± 2.9	3.5 ± 5.0	0.9 ± 4.1	1.3 ± 4.6
Mean response time					
MRT_{ON} (s)	ON	57.2 ± 15.9	64.9 ± 18.8	61.6 ± 17.3***	61.8 ± 15.9***
MRT_{OFF} (s)	OFF	39.7 ± 9.9	45.9 ± 11.8	41.9 ± 9.5***	42.9 ± 10.1***
Residual sum of squares					
(L^2 min^{-2})	ON	1.4 ± 1.3	25.0 ± 61.5	2.5 ± 2.2***	2.7 ± 2.5***
(L^2 min^{-2})	OFF	0.9 ± 0.9	8.4 ± 9.6	1.0 ± 0.9	1.5 ± 1.5***

$n = 20$ overall

*, **, and ***Significantly different from $\dot{V}O_2^{IND}$ time series (post hoc simple contrast) at the following significance levels of $p < 0.05$, $p < 0.01$, and $p < 0.005$, respectively. Notably, results obtained for the "Auchincloss" algorithm were not included in the statistical analysis of comparison between algorithms; see "Methods" for details

algorithms under investigation. The analysis carried out on the steady-state conditions as well as on the transients supports this result.

The validation of the performance of a new breath-by-breath O_2 uptake calculation algorithm requires, as a first step, to verify the congruence of results in steady-state conditions, where the fluctuations of the O_2 uptake around the average value also can be easily described. In turn, the most appropriate description of noise for the transient phases can only be obtained using a single repetition of the exercise transient in the moderate intensity domain.
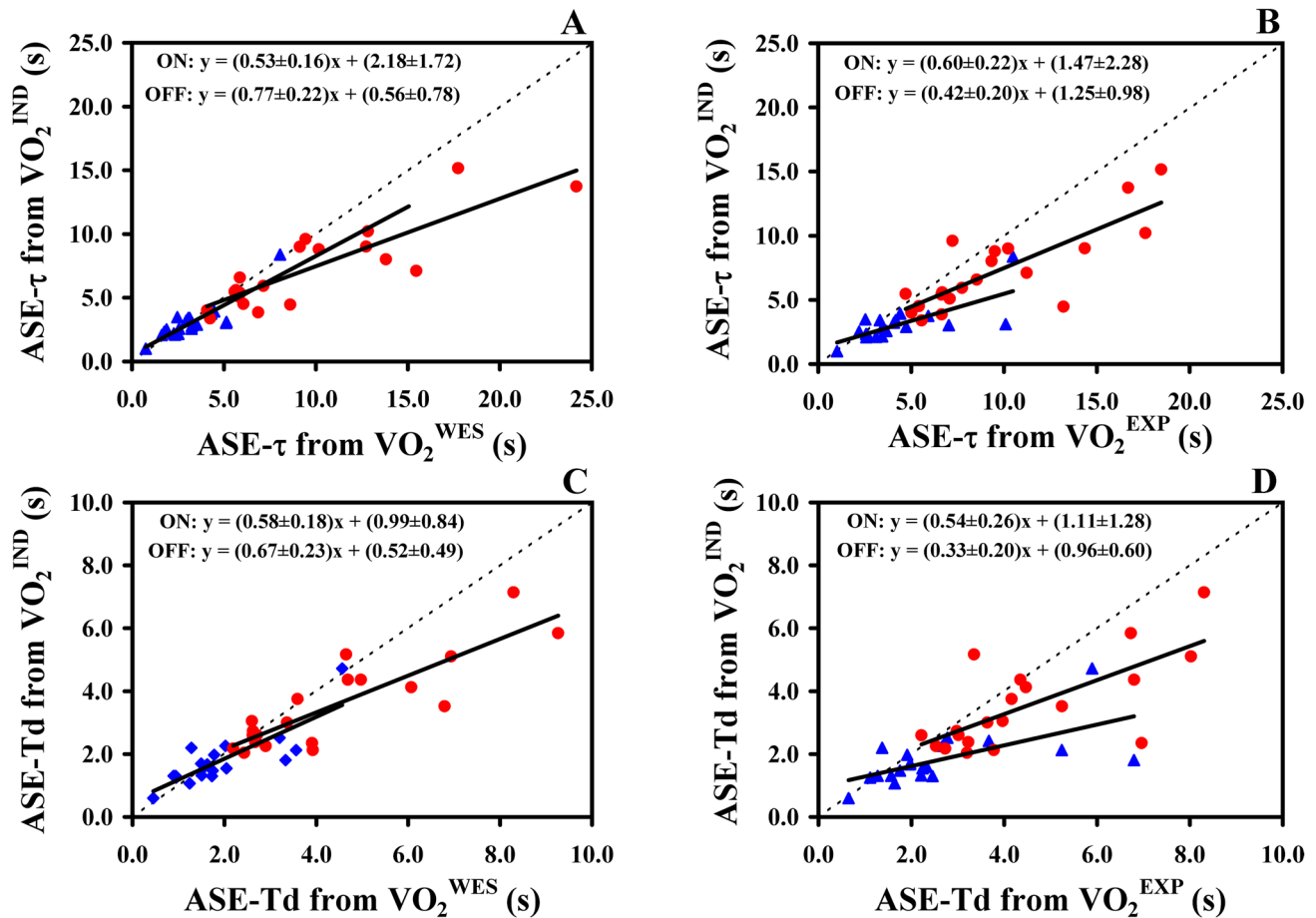
Fig. 6 Individual asymptotic standard error (ASE) values obtained from the non-linear regression procedure for the time constant (**a, b**) and for the time delays (**c, d**) using the O_2 uptake time series obtained with the "independent breath" algorithm are plotted as a function of the corresponding ASE values obtained using the "Wessel" algorithm (**a, c**) or the "expiration-only" algorithm (**b, d**). Data of the ON and OFF transients are plotted on the same panel. Data of all the 20 volunteers are plotted. Continuous line is the corresponding regression lines; dotted lines are the identity lines. The data corresponding to the two transients are illustrated with different symbols: filled circle≡ON transient; filled triangle≡OFF transient

Steady-state conditions

The experimental protocol adopted in the present investigation extended the results illustrated in our previous paper (Cettolo and Francescato 2018b). Indeed, we were able to study steady-state conditions ranging from an oxygen uptake of about 0.2 L min^{-1} at rest to the greatest value of about 1.8 L min^{-1} during loaded pedalling, in agreement with the O_2 uptakes investigated by other authors for the comparison of algorithms (Beaver et al. 1981; Busso and Robbins 1997; Auchincloss et al. 1966; Swanson 1980). The Bland–Altmann analysis carried out on this range of O_2 uptakes showed that the "independent breath" algorithm did not introduce systematic errors compared to the other algorithms. The bias of the average $\dot{V}O_2^{IND}$ values was in all cases negligible (< 1% of the grand average of the measured O_2 uptakes). The

95% limits of agreement, in the worst case (i.e., when the comparison was performed with the $\dot{V}O_2^{EXP}$ values), were < 11% of the grand average of the measured O_2 uptakes. The "Wessel" and "expiration-only" algorithms, as well as the "Auchincloss" algorithm have already been validated against the Douglas bags collection method (e.g., Capelli et al. 2001; Wilmore and Costill 1973). The "independent breath" algorithm yielded the same average O_2 uptake values at steady state; it can thus be concluded that this algorithm as well provide reliable oxygen uptake data.

The analysis of the standard deviations obtained for the data provided by the different algorithms showed that the "independent breath" algorithm resulted in a significantly lower variability of the O_2 uptakes. This is likely due to the fact that the "independent breath" algorithm takes into account the changes in lung stores for the calculations, thus resulting in a reduced fluctuation of the O_2 uptake data

(Capelli et al. 2011). In contrast, the great fluctuations in the gas-exchange data obtained by means of the "Auchincloss" algorithm should not surprise, because they were already observed by other authors (Cautero et al. 2003; di Prampero and Lafortuna 1989; Gimenez and Busso 2008; Goldman et al. 1986). All the algorithms had to cope with the same intrinsic noise due to the acquisition instrumentation and procedure, and used the same original flow and gas fraction traces to calculate the gas-exchange data; therefore, it should not surprise that the series of standard deviations were significantly correlated to each other. Nevertheless, if we assume that the slope of the regressions lines between the standard deviations obtained for the different algorithms represents the best overall estimator of reduced noise, the slope of < 0.69 (see Fig. 5) suggests that the noise of the O_2 uptakes yielded by the "independent breath" algorithm was at least 30% lower as compared to the other algorithms.

The exercise intensity was limited to the moderate domain to make us confident that all the volunteers were likely able to reach the steady-state condition during loaded pedalling, with the calculated averages and corresponding standard deviations having a meaning. Indeed, an a posteriori analysis on the time period from min 14:00 to min 16:00 (to exclude any transitory phase II $\dot{V}O_2$ data of the subject with the slowest response) showed that none of the slopes of the regression lines between $\dot{V}O_2$ data and time was statistically different from 0 ($t < 1.616$, $p > 0.11$ in all subjects). Higher exercise intensities could prevent the achievement of a steady-state condition in the O_2 uptake behaviour (Rossiter 2011), being above the individual's lactate threshold (Ward 2018), particularly so in the less fit volunteers. A higher steady-state condition could be obtained recruiting highly trained volunteers; under these conditions, however, the actual effects of noise could be masked.

The transient phases

The kinetic parameters obtained in the present investigation might be inadequate for physiological inferences, since only one exercise transition was performed by the volunteers. Nevertheless, the analysis of only one transition avoided masking the effects of noise due to the superposition of repeated data sets.

For both ON and OFF transient phases, the kinetics of the O_2 uptake was significantly different when the algorithms at stake were used to provide the gas-exchange data. The $\dot{V}O_2^{IND}$ time series resulted in (1) a significantly shorter mean response time for both transients; (2) a shorter time delay in the ON transient; and (3) a faster time constant of the OFF transient. Our results, however, are in line with the notion that the changes in the lung gas stores are expected in particular during the transient phases and that a correction for them results in a reduction of the

inherent O_2 uptake fluctuations, usually speeding up the response (Capelli et al. 2011). The faster response for the $\dot{V}O_2^{IND}$ compared to the $\dot{V}O_2^{WES}$ during the ON transient is in agreement with similar results reported by Cautero et al. (2002), who, however, used a unique reference gas fraction throughout in their implementation of Grønlund's approach (1984). For the OFF transient, to the best of our knowledge, we are the first to illustrate the comparison of the kinetic parameters obtained using gas-exchange data yielded by different algorithms.

Table 2 and Fig. 6 show that the use of the different algorithms at stake yielded, for both transients, significantly lower average RSS values and ASEs' values for both the time constant and the start time of signal change when using the IND algorithm, suggesting that also during the transient phase, the $\dot{V}O_2^{IND}$ time series were less noisy.

To make the non-linear regression procedure more robust (Motulsky and Ransnas 1987), no data were discarded for the transient analysis and a mono-exponential model was used to assess the kinetic parameters of the overall responses, including the estimate of the time delay. Indeed, a mono-exponential model with the time delay "fixed" to 0, although providing a similar estimate for the mean response time of the kinetics, would not allow us to depict the origin of the differences in the overall response. Moreover, we are aware that, to focus on the phase II, the analysis of the O_2 uptake transient phases is commonly performed excluding from the fitting window the data pertaining to the first 20 s (or less when baseline is higher than rest) starting from the change in workload (Benson et al. 2017). Accordingly, we evaluated results also for this procedure, excluding up to 20 s (in steps of 5 s) from the fitting window. In all cases, the above-described trends for the kinetic parameters, corresponding ASEs and RSS values were maintained. Nevertheless, dispersion of all these data was increased, thus decreasing the statistical significance of the differences (data not shown).

The exercise protocol adopted in the present work was not appropriate for the use of a double exponential model to estimate the kinetic parameters of both phase I and phase II. Indeed, the increased baseline O_2 uptake, due to the zero-load pedalling period, reduced the cardiodynamic phase I duration (Benson et al. 2017) and likely also its intensity. This condition, associated with the moderate exercise intensity, made it difficult to obtain reasonable results for the kinetic parameters of both phases (data not shown).

The adopted moderate intensity protocol might be interpreted as a limitation of the present investigation, since larger steps might induce important changes in the FO_2/FN_2 ratio in two subsequent breaths. Nevertheless, the "independent breath" algorithm, which deals with each breath by its own, was specifically designed to avoid loss of breaths in the calculations, even when large changes in the FO_2/FN_2

ratio occur, as those induced by the hyperventilation protocol we adopted in our previous work (Cettolo and Francescato 2018b).

Finally, the above results are of importance taking in mind that transient phases are even more often investigated to identify putative contributors to exercise tolerance not only in sport but also in health and disease (Ward 2018).

Possible practical implications of the reduced noise

The following lines try to describe the possible advantages of the use of the "independent breath" algorithm, which has been shown to be associated with a reduced noise.

The investigation of the $\dot{V}O_2$ kinetics is usually carried out by requiring volunteers to repeat the same transition more times to enhance the signal-to-noise ratio by assembling together the obtained $\dot{V}O_2$ time series. This procedure allows making smaller the ASE of the estimated kinetic parameters, in turn making narrower also the asymptotic confidence limits (Francescato et al. 2014a). Indeed, it has already been shown that assembling N repeated transitions allows decreasing the ASE as follows:

$$\text{ASE}_d \approx \frac{\text{ASE}_m}{\sqrt{N}}, \tag{6}$$

where ASE_m is the value obtained for only one repetition and ASE_d is the desired value (Francescato et al. 2014b).

It can be speculated that the use of the "independent breath" algorithm will likely allow the investigators to reduce the number of repetitions necessary to obtain the desired width of the confidence intervals for the estimated kinetic parameters. Applying the above equation to two theoretical algorithms, A and B, the reduction in the number of required repetitions to obtain the same desired ASE (and consequent confidence limits) can be calculated as

$$N_A \approx \left(\frac{\text{ASE}_{mA}}{\text{ASE}_{mB}} \right)^2 \cdot N_B, \tag{7}$$

where the subscripts A and B refer to the two different $\dot{V}O_2$ calculation algorithms. The slope of the regression line between corresponding ASE values can be taken as a proxy of the $\text{ASE}_{mA}/\text{ASE}_{mB}$ ratio. In the present investigation, for the time constant of the ON transient, the slope obtained between the ASE values of $\dot{V}O_2^{\text{IND}}$ and of $\dot{V}O_2^{\text{EXP}}$ (or $\dot{V}O_2^{\text{WES}}$) time series is < 0.60, which yields a reduction factor of $(0.60)^2 = 0.36$. This value allows expecting that the use of the "independent breath" algorithm might require a considerably reduced number of repetitions (about one-third). Nevertheless, taking into account also the results obtained on the steady-state conditions (30% reduction of variability in terms of standard deviation when using IND), we believe

that it is more prudent to state that only half of the repetitions are required to obtain the same width of confidence limits for τ_{ON} as compared to the WES and EXP algorithms. It should be remembered here, however, that the above are only theoretical speculations.

Strengths and limitations

The aim of the present work was the comparison of the O_2 uptake data provided by the various algorithms at stake, focusing in particular on the noise of the data. Consequently, we recruited healthy, moderately active volunteers of both genders, showing a wide range of ages, and of different training levels, who were asked to perform only one repetition of the exercise protocol. This choice allowed us to investigate different breathing patterns and kinetic behaviours under conditions of low signal-to-noise ratio. The moderate intensity exercise domain and only one repetition for the comparison among algorithms are in agreement with the previous similar papers (Beaver et al. 1981; Busso and Robbins 1997; Auchincloss et al. 1966; Swanson 1980). We believed that, in the present stage of evaluation of the "independent breath" algorithm, it was meaningless to ask volunteers repeating more times the same protocol, although we are aware that the obtained physiological parameters should be taken with some caution because of the explicitly searched low signal-to-noise ratio. Conversely, the adopted protocol allowed us to compare the algorithms at stake using statistical parameters as standard deviations and ASE, which can be appropriately used as indicators of the noise level.

The algorithms at stake were applied on the same gas fractions and flow digital traces, using the same calculation routines, allowing us to eliminate differences related to the devices running the different algorithms (e.g., methods used to synchronize flow and gas signals, errors in sensor calibrations) and the algorithms were subjected to the same systematic errors derived from the acquisition of the original data.

It remains to be determined whether the proposed algorithm will still produce less noisy data in higher exercise intensity domains or in more complex exercise protocols. In addition, the theoretical reduction of the number of repeats necessary for kinetic evaluation has to be confirmed experimentally. Finally, the "independent breath" approach should be evaluated under pathological conditions, e.g., patients suffering from respiratory diseases.

Conclusions

The "independent breath" algorithm is suitable for real-time calculation of breath-by-breath gas-exchange data, taking into account the changes in lung gas stores. Results of the present investigation show that the "independent breath"

algorithm yielded congruent average O$_2$ uptake values at steady state and resulted in a prompter response to changes in the O$_2$ requirement during transients. The greatest impact of the "independent breath" algorithm, however, is the reduction in the overall noise of the breath-by-breath O$_2$ uptake data, which might result in a halving of the number of repeated trials required to obtain the same width of the confidence limits when assessing the kinetic parameters of the ON transient.

Author contributions CV and FMP equally contributed in conception and design of the experiments; both performed the experiments, analysed the data, and wrote the paper. Both authors read and approved the final version of the manuscript.

References

Auchincloss JHJ, Gilbert R, Baule GH (1966) Effect of ventilation on oxygen transfer during early exercise. J Appl Physiol 21:810–818

Bates D, Watts D (1988) Nonlinear regression analysis and its applications. Wiley, New York

Beaver WL, Lamarra N, Wasserman K (1981) Breath-by-breath measurement of true alveolar gas exchange. J Appl Physiol 51:1662–1675

Benson A, Bowen T, Ferguson C, Murgatroyd S, Rossiter HB (2017) Data collection, handling and fitting strategies to optimize accuracy and precision of oxygen uptake kinetics estimation from breath-by-breath measurements. J Appl Physiol 123:227–242. https://doi.org/10.1152/japplphysiol.00988.2016

Bland JM, Altman DG (1986) Statistical methods for assessing agreement between two methods of clinical measurement. Lancet 1:307–310

Busso T, Robbins PA (1997) Evaluation of estimates of alveolar gas exchange by using a tidally ventilated nonhomogenous lung model. J Appl Physiol 82:1963–1971

Capelli C, Cautero M, di Prampero PE (2001) New perspectives in breath-by-breath determination of alveolar gas exchange in humans. Pflugers Arch 441:566–577

Capelli C, Cautero M, Pogliaghi S (2011) Algorithms, modelling and VO$_2$ kinetics. Eur J Appl Physiol 111:331–342. https://doi.org/10.1007/s00421-010-1396-8

Cautero M, Beltrami AP, di Prampero PE, Capelli C (2002) Breath-by-breath alveolar oxygen transfer at the onset of step exercise in humans: methodological implications. Eur J Appl Physiol 88:203–213. https://doi.org/10.1007/s00421-002-0671-8

Cautero M, di Prampero PE, Capelli C (2003) New acquisitions in the assessment of breath-by-breath alveolar gas transfer in humans. Eur J Appl Physiol 90:231–241. https://doi.org/10.1007/s00421-003-0951-y

Cettolo V, Francescato MP (2015) Assessment of breath-by-breath alveolar gas exchange: an alternative view of the respiratory cycle. Eur J Appl Physiol 115:1897–1904. https://doi.org/10.1007/s00421-015-3169-x

Cettolo V, Francescato MP (2018a) Effects of abrupt changes in lung gas stores on the assessment of breath-by-breath gas exchange. Clin Physiol Funct Imaging 38:491–496. https://doi.org/10.1111/cpf.12444

Cettolo V, Francescato MP (2018b) Assessing breath-by-breath alveolar gas exchange: is the contiguity in time of breaths mandatory? Eur J Appl Physiol 118:1119–1130. https://doi.org/10.1007/s00421-018-3842-y

di Prampero PE, Lafortuna CL (1989) Breath-by-breath estimate of alveolar gas transfer variability in man at rest and during exercise. J Physiol 415:459–475

Fowler WS (1948) Lung function studies. II. The respiratory dead space. J Appl Physiol 154:405–416. https://doi.org/10.1152/ajplegacy.1948.154.3.405

Francescato MP, Cettolo V, Bellio R (2014a) Assembling more O$_2$ uptake responses: is it possible to merely stack the repeated transitions? Respir Physiol Neurobiol 200:46–49. https://doi.org/10.1016/j.resp.2014.06.004

Francescato M, Cettolo V, Bellio R (2014b) Confidence intervals for the parameters estimated from simulated O$_2$ uptake kinetics: effects of different data treatments. Exp Physiol 99:187–195. https://doi.org/10.1113/expphysiol.2013.076208

Gimenez P, Busso T (2008) Implications of breath-by-breath oxygen uptake determination on kinetics assessment during exercise. Respir Physiol Neurobiol 162:238–241. https://doi.org/10.1016/j.resp.2008.07.004

Goldman E, Dzwonczyk R, Yadagani V (1986) Evaluation of four methods for estimating breath-by-breath exchange of O$_2$ and CO$_2$. IEEE Trans Biomed Eng BME 33:524–526

Golja P, Cettolo V, Francescato MP (2018) Calculation algorithms for breath-by-breath alveolar gas exchange: the unknowns! Eur J Appl Physiol 118:1869–1876. https://doi.org/10.1007/s00421-018-3914-z

Grønlund J (1984) A new method for breath-to-breath determination of oxygen flux across the alveolar membrane. Eur J Appl Physiol 52:167–172

Motulsky HJ, Ransnas LA (1987) Fitting curves to data using nonlinear regression: a practical and nonmathematical review. FASEB J 1:365–374

R Core Team (2015) R: a language and environment for statistical computing (vs. 3.2.2). R Foundation for Statistical Computing, Wien

Roberts CM, MacRae KD, Winning AJ, Adams L, Seed WA (1991) Reference values and prediction equations for normal lung function in a non-smoking white urban population. Thorax 46:643–650

Roecker K, Prettin S, Sorichter S (2005) Gas exchange measurements with high temporal resolution: the breath-by-breath approach. Int J Sports Med 26:S11–S18. https://doi.org/10.1055/s-2004-830506

Rossiter HB (2011) Exercise: kinetic considerations for gas exchange. Compr Physiol 1:203–244. https://doi.org/10.1002/cphy.c090010

Swanson G (1980) Breath-to breath considerations for gas exchange kinetics. In: Cerretelli P, Whipp BJ (eds) Exercise bioenergetics and gas exchange. Elsevier, Amsterdam, pp 211–222

Ward SA (2018) Open-circuit respirometry: real-time, laboratory-based systems. Eur J Appl Physiol 118:875–898. https://doi.org/10.1007/s00421-018-3860-9

Wessel H, Stout R, Bastanier C, Paul M (1979) Breath-by-breath variation of FRC: effect on VO$_2$ and VCO$_2$ measured at the mouth. J Appl Physiol Respir Environ Exerc Physiol 46:1122–1126

Wilmore JH, Costill DL (1973) Adequacy of the Haldane transformation in the computation of exercise VO$_2$ in man. J Appl Physiol 35:85–89